

UNCLASSIFIED

Defense Technical Information Center
Compilation Part Notice

ADP012063

TITLE: High-Order Nystrom Method for Computing Waveguide Modes

DISTRIBUTION: Approved for public release, distribution unlimited

This paper is part of the following report:

TITLE: Applied Computational Electromagnetics Society Journal. Volume 17, Number 1

To order the complete compilation report, use: ADA399939

The component part is provided here to allow users access to individually authored sections of proceedings, annals, symposia, etc. However, the component should be considered within the context of the overall compilation report and not as a stand-alone technical report.

The following component part numbers comprise the compilation report:

ADP012055 thru ADP012066

UNCLASSIFIED

High-order Nyström Method for Computing Waveguide Modes

John J. Ottusch and Stephen M. Wandzura

HRL Laboratories, LLC
3011 Malibu Canyon Road
Malibu, CA 90265
ottusch@hrl.com

Abstract—We report a novel method for accurately computing the modes of an arbitrarily-shaped hollow waveguide. Our method uses a point-based (Nyström) discretization of an integral operator over the waveguide aperture to compute the modes.

I. INTRODUCTION

This paper describes a technique for numerically computing the modes of an arbitrarily-shaped cylindrical waveguide with perfectly-conducting walls and an isotropic, homogeneous core. The method is different from standard methods in that we formulate the problem in terms of the eigenfunctions of an integral operator over the waveguide aperture and it is unique in that we employ a high-order, point-based (Nyström) discretization to obtain numerical solutions.

The Nyström method is a method for solving integral equations. In contrast to a method of moments discretization, a Nyström discretization of a function on a surface S is simply a tabulation of function values at a discrete set of points on S . Integrals are approximated by weighted sums of function evaluations. Specifically, we approximate the integral of a function $f(x)$ as

$$\int dx f(x) \simeq \sum_{i=1}^N \omega_i f(x_i), \quad (1)$$

where x_i is the i^{th} abscissa of an N -point, high-order quadrature rule and ω_i is the associated quadrature weight.

The conventional Nyström method is a simple and efficient method for solving integral equations with non-singular kernels. When the integral kernel is singular (as is generally the case for Green functions), one needs to introduce *local corrections* in order to compensate for the fact that a quadrature rule for regular functions cannot integrate singular functions with high-order accuracy. Further details regarding local corrections and their use in the Nyström method for solving scattering problems may be found in [1].

The modes of an isotropic, homogeneous-core cylindrical waveguide with perfectly conducting walls can be classified [2] into three categories — transverse magnetic (TM), transverse electric (TE), and transverse electromagnetic (TEM). Modes in each category are related to the modes of a scalar waveguide problem. The TM (TE) modes are derivable from the scalar modes of the same waveguide assuming Dirichlet (Neumann) boundary conditions on its walls. The TEM modes are derivable from solutions to the $2d$ Laplace equation on a cross section of the guide.

The arrangement of the remainder of the paper is as follows: section II describes how to obtain eigenmodes and eigenvalues for the scalar waveguide problem with Dirichlet or Neumann boundary conditions; section III describes how to solve the $2d$ Laplace equation inside the waveguide aperture; section IV describes a method for computing the vector waveguide modes from the scalar traveling modes and $2d$ electrostatic modes; and, finally, in section V we present some results obtained from a software implementation of these methods.

II. SCALAR WAVEGUIDE MODES

The scalar waveguide modes $u_n(\mathbf{x})$ satisfy the $2d$ scalar wave equation

$$(\nabla_{\perp}^2 + k^2 - \beta_n^2) u_n(\mathbf{x}) = 0 \quad (2)$$

inside the waveguide aperture W and the correct boundary conditions on its boundary ∂W . They are also eigenfunctions of the H operator [3] defined as

$$H(\mathbf{x}, \mathbf{x}') \equiv \sum_n \frac{Z_n}{ik} u_n(\mathbf{x}) u_n(\mathbf{x}'). \quad (3)$$

In these equations,

$$Z_n = \frac{k}{\beta_n} \quad (4)$$

is the modal impedance, k is the free-space propagation constant, and β_n is the propagation constant for the n^{th} waveguide mode.

Using the fact that the modes form a complete and orthonormal set of real functions on W , one can show that the function \tilde{G} defined by

$$\tilde{G}(\mathbf{x}, \mathbf{x}'') \equiv \int_W ds' H(\mathbf{x}, \mathbf{x}') H(\mathbf{x}', \mathbf{x}''), \quad (5)$$

is the Green function appropriate to the inside of the waveguide because it obeys the wave equation $(\nabla_{\perp}^2 + k^2) \tilde{G}(\mathbf{x}, \mathbf{x}'') = -\delta^{(2)}(\mathbf{x}, \mathbf{x}'')$ inside W and the correct boundary conditions on ∂W . Furthermore, the eigenfunctions of the integral operator

$$\int_W ds'' \tilde{G}(\mathbf{x}, \mathbf{x}'') = \sum_n \left(\frac{Z_n}{ik} \right)^2 u_n(\mathbf{x}) \int_W ds' u_n(\mathbf{x}') \quad (6)$$

are the modes of the waveguide and the eigenvalue corresponding to the n^{th} mode $u_n(\mathbf{x})$ is

$$\left(\frac{Z_n}{ik} \right)^2 = -\frac{1}{\beta_n^2}. \quad (7)$$

Therefore, our procedure for computing the scalar traveling modes of a waveguide will consist of first computing a discretized representation of the integral operator $\int_W ds'' \tilde{G}(\mathbf{x}, \mathbf{x}'')$ and then using a numerical eigenvalue routine to determine discretized representations (of a finite set) of the modes and the corresponding propagation constants. The remainder of this section describes a method for obtaining discretized representations of $\int_W ds'' \tilde{G}(\mathbf{x}, \mathbf{x}'')$ with Dirichlet or Neumann boundary conditions on ∂W .

Start with a solution to the inhomogeneous (transverse) wave equation $(\nabla_{\perp}^2 + k^2) G(\mathbf{x}, \mathbf{x}') = -\delta^{(2)}(\mathbf{x}, \mathbf{x}')$. We will use

$$G(\mathbf{x}, \mathbf{x}') = -\frac{1}{4} Y_0(k|\mathbf{x} - \mathbf{x}'|), \quad (8)$$

where Y_0 is the second kind Bessel function of order zero. To this solution we can always add solutions $F(\mathbf{x}, \mathbf{x}')$ to the homogeneous wave equation $(\nabla_{\perp}^2 + k^2) F(\mathbf{x}, \mathbf{x}') = 0$. Our objective is to find a solution F that makes

$$\tilde{G}(\mathbf{x}, \mathbf{x}') = G(\mathbf{x}, \mathbf{x}') + F(\mathbf{x}, \mathbf{x}') \quad (9)$$

obey the boundary conditions on ∂W . Unlike the Green function for $2d$ scattering in an unbounded region, this Green function is real valued.

A. Dirichlet Case

Since we care only about \tilde{G} inside W , we can arrange any distribution of charges σ outside of W to make \tilde{G} obey the boundary conditions on ∂W . The simplest solution is to put them on an artificial boundary Γ that is outside ∂W by an infinitesimal distance. Then

$$F(\mathbf{x}, \mathbf{x}') \equiv \int_{\Gamma} dl'' G(\mathbf{x}, \mathbf{x}'') \sigma(\mathbf{x}'', \mathbf{x}') \quad (10)$$

obeys

$$\begin{aligned} & (\nabla_{\perp}^2 + k^2) F(\mathbf{x}, \mathbf{x}') \\ &= \int_{\Gamma} dl'' (\nabla_{\perp}^2 + k^2) G(\mathbf{x}, \mathbf{x}'') \sigma(\mathbf{x}'', \mathbf{x}') = 0 \end{aligned} \quad (11)$$

since $(\nabla_{\perp}^2 + k^2) G(\mathbf{x}, \mathbf{x}'') = 0$ for all $\mathbf{x} \in W$ and $\mathbf{x}'' \in \Gamma$. Taking the limit as $\Gamma \rightarrow \partial W$ we get

$$\tilde{G}(\mathbf{x}, \mathbf{x}') = G(\mathbf{x}, \mathbf{x}') + \int_{\partial W} dl'' G(\mathbf{x}, \mathbf{x}'') \sigma(\mathbf{x}'', \mathbf{x}'). \quad (12)$$

A simple interpretation of this equation is as follows: $\sigma(\mathbf{x}'' \in \partial W, \mathbf{x}' \in W)$ is the charge distribution induced on the walls of the waveguide by a unit charge at $\mathbf{x}' \in W$; the total potential at $\mathbf{x} \in \partial W$ is the sum of the potential from the original unit charge, namely $G(\mathbf{x}, \mathbf{x}')$, and the potential produced by the induced charge distribution on the waveguide walls, namely

$$\int_{\partial W} dl'' G(\mathbf{x}, \mathbf{x}'') \sigma(\mathbf{x}'', \mathbf{x}'). \quad (13)$$

In the Dirichlet case, the total potential must vanish everywhere on ∂W . To enforce this condition, we will demand that the inner product of the potential on ∂W with each function $f_k(\mathbf{x} \in \partial W)$ from a suitable set of testing functions must vanish, i.e.,

$$\begin{aligned} 0 &= \int_{\partial W} dl f_k(\mathbf{x}) G(\mathbf{x}, \mathbf{x}') \\ &+ \int_{\partial W} dl f_k(\mathbf{x}) \int_{\partial W} dl'' G(\mathbf{x}, \mathbf{x}'') \sigma(\mathbf{x}'', \mathbf{x}') \end{aligned} \quad (14)$$

for every point $\mathbf{x}' \in W$.

We can write this condition in matrix form as

$$0 = f^{\partial W} \Omega^{\partial W} (G^{\partial W, W} + G^{\partial W, \partial W} \Omega^{\partial W} \Sigma^{\partial W, W}) \quad (15)$$

where $\Sigma^{\partial W, W}$ represents the discretized form of σ and $G^{\partial W, \partial W}$ and $G^{\partial W, W}$ are discretized representations of the kernel G with local corrections [1]. $\Omega^{\partial W}$ is a diagonal matrix of quadrature weights for integrals over ∂W . [In general, our notation involving W and ∂W superscripts is meant to indicate the domain(s) of the coordinate variable(s). For diagonal quadrature weight matrices Ω , only one superscript is used for notational compactness with the understanding that the two domains are always the same.] Since $f^{\partial W}$ is arbitrary, the solution to (15) is

$$\Sigma^{\partial W, W} = - (G^{\partial W, \partial W} \Omega^{\partial W})^{-1} G^{\partial W, W}, \quad (16)$$

which means that the discretized form of $\int_W ds'' \tilde{G}(\mathbf{x}, \mathbf{x}'')$ is

$$G^{W, W} \Omega^W - G^{W, \partial W} (G^{\partial W, \partial W})^{-1} G^{\partial W, W} \Omega^W. \quad (17)$$

B. Neumann Case

As in the Dirichlet case, we arrange sources on Γ in just the right amount to make the total potential obey the boundary conditions on ∂W . In the Neumann case, however, a dipole distribution μ has some advantages over a charge distribution¹.

The potential at any point $\mathbf{x} \in W$ due to a dipole distribution μ on Γ is

$$F(\mathbf{x}, \mathbf{x}') = \int_{\Gamma} dl'' (\hat{\mathbf{e}}'' \cdot \nabla'' G(\mathbf{x}, \mathbf{x}'')) \mu(\mathbf{x}'', \mathbf{x}'), \quad (18)$$

where $\hat{\mathbf{e}}''$ is the unit normal to ∂W at \mathbf{x}'' in the plane of, but pointing away from, W . For the same reason as before, F obeys the homogeneous wave equation whenever $\mathbf{x} \in W$. The edge normal derivative of F at $\mathbf{x} \in \Gamma$ is

$$\hat{\mathbf{e}} \cdot \nabla F(\mathbf{x}, \mathbf{x}') = (\hat{\mathbf{e}} \cdot \nabla) \int_{\Gamma} dl'' (\hat{\mathbf{e}}'' \cdot \nabla'' G(\mathbf{x}, \mathbf{x}'')) \mu(\mathbf{x}'', \mathbf{x}'). \quad (19)$$

The normal derivative of a dipole layer potential is continuous across the boundary so we can take the limit $\Gamma \rightarrow \partial W$, replacing Γ by ∂W in the above expression.

In the Neumann case, the edge normal derivative of the total potential must vanish everywhere on ∂W . We will demand that the inner product of the edge normal derivative of the potential on ∂W with each function from a suitable set of testing functions must vanish. In other words, for each testing function $f_k(\mathbf{x} \in \partial W)$, we require that

$$0 = \int_{\partial W} dl f_k(\mathbf{x}) (\hat{\mathbf{e}} \cdot \nabla G(\mathbf{x}, \mathbf{x}')) + \int_{\partial W} dl f_k(\mathbf{x}) (\hat{\mathbf{e}} \cdot \nabla) \int_{\partial W} dl'' (\hat{\mathbf{e}}'' \cdot \nabla'' G(\mathbf{x}, \mathbf{x}'')) \mu(\mathbf{x}'', \mathbf{x}') \quad (20)$$

for every point $\mathbf{x}' \in W$.

We can write this in matrix form as

$$0 = f^{\partial W} \Omega^{\partial W} \left((\hat{\mathbf{e}} \cdot \nabla G)^{\partial W, W} + [(\hat{\mathbf{e}} \cdot \nabla) (\hat{\mathbf{e}}'' \cdot \nabla'' G)]^{\partial W, \partial W} \Omega^{\partial W} M^{\partial W, W} \right) \quad (21)$$

where $M^{\partial W, W}$ represents the discretized form of μ , and $[(\hat{\mathbf{e}} \cdot \nabla) (\hat{\mathbf{e}}'' \cdot \nabla'' G)]^{\partial W, \partial W}$ and $(\hat{\mathbf{e}} \cdot \nabla G)^{\partial W, W}$ are discretized representations of the corresponding edge normal

¹The problem with using a charge distribution in the Neumann case is that it diverges at acute angle corners, such as in a square waveguide. A 1d quadrature rule designed to integrate regular functions will not be high order for such a charge distribution. For waveguide apertures with smooth edges, such as a circular guide, this is not a problem and using a charge distribution may well better since the integral operator is second kind.

When using a charge distribution σ for the Neumann case, beware of the fact that the limit of $\int_{\Gamma} dl'' (\hat{\mathbf{e}} \cdot \nabla G(\mathbf{x}, \mathbf{x}'')) \sigma(\mathbf{x}'', \mathbf{x}')$ as $\Gamma \rightarrow \partial W$ is $\frac{1}{2} \sigma(\mathbf{x}, \mathbf{x}') + \int_{\partial W} dl'' (\hat{\mathbf{e}} \cdot \nabla G(\mathbf{x}, \mathbf{x}'')) \sigma(\mathbf{x}'', \mathbf{x}')$.

derivative operators with local corrections. Ω^W and $\Omega^{\partial W}$ are diagonal matrices of quadrature weights for integrals over W and ∂W , respectively. The solution to (21) is

$$M^{\partial W, W} = - \left([(\hat{\mathbf{e}} \cdot \nabla) (\hat{\mathbf{e}}'' \cdot \nabla'' G)]^{\partial W, \partial W} \Omega^{\partial W} \right)^{-1} (\hat{\mathbf{e}} \cdot \nabla G)^{\partial W, W}, \quad (22)$$

which means that the discretized form of $\int_W ds'' \tilde{G}(\mathbf{x}, \mathbf{x}'')$ in the Neumann case is

$$G^{W, W} \Omega^W - (\hat{\mathbf{e}} \cdot \nabla G)^{\partial W, W} \left([(\hat{\mathbf{e}} \cdot \nabla) (\hat{\mathbf{e}}'' \cdot \nabla'' G)]^{\partial W, \partial W} \right)^{-1} (\hat{\mathbf{e}} \cdot \nabla G)^{\partial W, W} \Omega^W. \quad (23)$$

III. SOLVING LAPLACE'S EQUATION IN W

When the waveguide aperture is multiply-connected, there exist non-trivial solutions to the 2d Laplace equation in W . Such solutions correspond to the TEM modes in the waveguide.

What follows is a procedure for computing the solution to the 2d Laplace equation in W for an arbitrary potential distribution on the boundaries. The same procedure has an obvious extension to 3d which could be used to solve electrostatic problems inside multiply-connected cavities.

For a given boundary value function $b(\mathbf{x} \in \partial W)$, we desire to find a function $\psi(\mathbf{x} \in W)$ that satisfies

$$\psi(\mathbf{x}) = b(\mathbf{x}) \text{ for } \mathbf{x} \in \partial W, \text{ and} \quad (24)$$

$$\nabla^2 \psi(\mathbf{x}) = 0 \text{ for } \mathbf{x} \in W. \quad (25)$$

The solution for $\psi(\mathbf{x})$ can be written as a 2d single-layer potential with an unknown source distribution

$$\psi(\mathbf{x}) = \int_{\partial W} dl' \log |\mathbf{x} - \mathbf{x}'| \sigma(\mathbf{x}'). \quad (26)$$

This potential automatically satisfies the second condition above because $\nabla^2 \log |\mathbf{x} - \mathbf{x}'| = 0$ for $\mathbf{x} \in W$ and $\mathbf{x}' \in \partial W$. The single-layer potential density $\sigma(\mathbf{x}')$ is determined by the condition that $\psi(\mathbf{x}) = b(\mathbf{x})$ on the boundary, i.e.,

$$\int_{\partial W} dl' \log |\mathbf{x} - \mathbf{x}'| \sigma(\mathbf{x}') = b(\mathbf{x}). \quad (27)$$

If $L^{\partial W, \partial W}$ and $L^{W, \partial W}$ are the discretized representations of $\log |\mathbf{x} - \mathbf{x}'|$ (with local corrections) for $\mathbf{x} \in \partial W$ and $\mathbf{x} \in W$, respectively, and Ψ^W , $\Sigma^{\partial W}$, and $B^{\partial W}$ are the discretized representations of $\psi(\mathbf{x})$, $\sigma(\mathbf{x})$ and $b(\mathbf{x})$, respectively, then

$$L^{\partial W, \partial W} \Omega^{\partial W} \Sigma^{\partial W} = B^{\partial W}, \quad (28)$$

and the solution for Ψ^W becomes

$$\Psi^W = L^{W, \partial W} \Omega^{\partial W} \Sigma^{\partial W} = L^{W, \partial W} (L^{\partial W, \partial W})^{-1} B^{\partial W}. \quad (29)$$

To get TEM modes, W must be multiply connected, i.e.,

$$\partial W = \partial W_1 \cup \partial W_2 \dots \cup \partial W_n \quad (30)$$

where the ∂W_i are unconnected boundaries and $n \geq 2$. There is a TEM mode corresponding to each of the $n - 1$ independent boundary functions described by

$$b_{ik}(\mathbf{x}) = 0 \text{ for all } k \text{ except } k = i \quad (31)$$

$$b_{ii}(\mathbf{x}) = 1 \quad (32)$$

for $i = 1, 2, \dots, n - 1$.

IV. VECTOR WAVEGUIDE MODES

The transverse electric components of the TM, TE, and TEM vector waveguide modes are derivable from the scalar waveguide modes according to

$$\mathbf{u}_n^{TM}(\mathbf{x}) = \frac{\nabla \varphi_n}{\sqrt{k^2 - \beta_n^2}} \quad (33)$$

$$\mathbf{u}_n^{TE}(\mathbf{x}) = \frac{\hat{\mathbf{n}} \times \nabla \psi_n}{\sqrt{k^2 - \beta_n^2}} \quad (34)$$

$$\mathbf{u}_n^{TEM}(\mathbf{x}) \propto \nabla \zeta_n, \quad (35)$$

where φ_n , ψ_n , and ζ_n are the scalar Dirichlet, Neumann, and Laplace modes, respectively. The transverse magnetic component [2] is

$$\mathbf{H}_\perp = \pm Z_n^{-1} \hat{\mathbf{n}} \times \mathbf{E}_\perp, \quad (36)$$

where

$$Z_n = \sqrt{\frac{\mu}{\epsilon}} \times \begin{cases} \frac{\beta_n}{k} & \text{for } n \in TM \text{ modes} \\ 1 & \text{for } n \in TEM \text{ modes} \\ \frac{k}{\beta_n} & \text{for } n \in TE \text{ modes} \end{cases} \quad (37)$$

is the modal impedance and ϵ and μ are the dielectric constant and magnetic permeability, respectively.

We need discretized representations of the surface gradient to effect the transformation from scalar modes to vector modes given above. This section shows how to represent the surface gradient operator (on an arbitrary surface) in matrix form. Left multiplying a matrix representing a scalar surface function by the matrix representing the surface gradient produces a discretized representation of the surface gradient of the scalar function.

First consider the linear derivative operator. In the spirit of the high-order Nyström method, we will demand that the discretized derivative operator return exact results at a particular set of sample points for each function in a set of suitable functions. In other words, if we are given a set of points x_j on a curve C , then $\Delta_{ij} = \Delta(x_i, x_j)$ is a high-order discretized representation of the differential operator $\frac{d}{dx}$ at x_i on C if it is the

solution to the linear system

$$\sum_j \Delta(x_i, x_j) f_k(x_j) = \frac{df_k(x_i)}{dx}. \quad (38)$$

for suitable testing functions $f_k(x)$.

We can also make a connection with the Nyström method by re-expressing the derivative as an integral operator and applying the standard procedure [1] for computing local corrections. If we write the linear derivative of $f(x)$ on the curve C as

$$\frac{df(x)}{dx} = \frac{d}{dx} \int_C dx' \delta(x - x') f(x'), \quad (39)$$

then the discretized representation of the differential operator $\frac{d}{dx}$ on C is obtained by solving the linear system

$$\begin{aligned} & \sum_j \omega_j \tilde{\Delta}(x_i, x_j) f_k(x_j) \\ &= \left[\frac{d}{dx} \int_C dx' \delta(x - x') f_k(x') \right]_{x=x_i} = \frac{df_k(x_i)}{dx} \end{aligned} \quad (40)$$

for $\tilde{\Delta}(x_i, x_j)$ using suitable testing functions $f_k(x)$. Clearly, $\tilde{\Delta}$ and Δ are related by $\tilde{\Delta}\Omega = \Delta$. The only difference between this linear system and the local correction linear system in [1] is that computing the right hand side of (40) only requires evaluating derivatives of the testing functions at the sample points instead of evaluating inner products of the kernel with testing functions.

We have encountered operators similar to this in scattering problems before. The hypersingular operators $(\mathbf{n} \cdot \nabla) \int ds' (\mathbf{n}' \cdot \nabla') G(x, x')$ and $(\mathbf{n} \times \nabla) \int ds' (\mathbf{n}' \times \nabla') G(x, x')$, which appear in boundary integral formulations of scalar and electromagnetic scattering, respectively, are pseudo-differential operators. Like these operators, the discretized gradient operator must be used with extreme caution (and avoided whenever possible) because it tends to amplify rather than attenuate numerical "noise".

Now consider surface derivative operators. Let $\hat{\mathbf{t}}_1(\mathbf{x})$ and $\hat{\mathbf{t}}_2(\mathbf{x})$ be independent unit tangent vectors on the surface S . By analogy with the linear derivative operator, we obtain a locally corrected matrix representation $\Delta_\mu(\mathbf{x}_i, \mathbf{x}_j)$ of the surface gradient operator $\hat{\mathbf{t}}_\mu \cdot \nabla$ on S by solving the linear system

$$\sum_j \Delta_\mu(\mathbf{x}_i, \mathbf{x}_j) f_k(\mathbf{x}_j) = \hat{\mathbf{t}}_\mu(\mathbf{x}_i) \cdot \nabla f_k(\mathbf{x}_i) \quad (41)$$

with $\mu = 1, 2$ using suitable testing functions $f_k(x)$. If these testing functions afford a high-order approximation to a scalar function $\psi(x)$ on S , then the vector $\Delta_\mu \Psi$ represents a high-order approximation to $\hat{\mathbf{t}}_\mu(\mathbf{x}) \cdot \nabla \psi(\mathbf{x})$, with $(\Delta_\mu)_{ij} \equiv \Delta_\mu(\mathbf{x}_i, \mathbf{x}_j)$ and $\Psi_i \equiv \psi(\mathbf{x}_i)$.

The matrix representation of $\hat{\mathbf{n}} \times \nabla$ is obtained by replacing $\hat{\mathbf{t}}_\mu(\mathbf{x}_i) \cdot \nabla$ with $\hat{\mathbf{t}}_\mu(\mathbf{x}_i) \cdot (\hat{\mathbf{n}} \times \nabla)$ in (41).

TABLE I

COMPUTED AND EXACT EIGENVALUES ($\beta_{m,n}/k$) FOR A $1.1\lambda \times 0.75\lambda$ WAVEGUIDE SATISFYING DIRICHLET BOUNDARY CONDITIONS

4 x 4	6 x 6	8 x 8	Exact	m	n
0.592201	0.590741	0.590716	0.590715	1	1
0.512091i	0.520366i	0.520471i	0.520472i	2	1
0.969128i	0.991772i	0.992159i	0.992164i	1	2
1.219852i	1.159101i	1.142176i	1.141906i	3	1
1.629548i	1.265721i	1.266571i	1.266580i	2	2
1.997986i	1.574208i	1.624191i	1.623971i	3	2
2.080501i	1.637739i	1.648007i	1.658382i	4	1
2.309772i	1.817060i	1.791106i	1.790701i	1	4
2.546563i	1.929628i	1.956519i	1.956130i	2	4
2.694088i	1.981966i	2.010146i	2.020783i	4	2
3.010537i	2.237905i	2.204944i	2.147029i	5	1
3.114740i	2.385630i	2.279746i	2.204428i	3	3
3.321089i	2.444649i	2.497769i	2.437841i	5	2
3.469637i	2.503110i	2.501035i	2.511132i	4	3
3.642493i	2.696163i	2.537604i	2.513508i	1	4
3.744043i	2.836216i	2.560426i	2.633924i	2	4

TABLE II

COMPUTED AND EXACT EIGENVALUES ($\beta_{m,n}/k$) FOR A $1.1\lambda \times 0.75\lambda$ WAVEGUIDE SATISFYING NEUMANN BOUNDARY CONDITIONS

4 x 4	6 x 6	8 x 8	Exact	m	n
0.889957	0.890835	0.890726	0.890724	1	0
0.745280	0.745429	0.745358	0.745356	0	1
0.587578	0.590805	0.590715	0.590715	1	1
0.443112	0.412701	0.416826	0.416598	2	0
0.507053i	0.527063i	0.520106i	0.520472i	2	1
0.758857i	0.883037i	0.881869i	0.881917i	0	2
0.919138i	0.922549i	0.925573i	0.927094i	3	0
0.928154i	0.994163i	0.992079i	0.992164i	1	2
1.028942i	1.141903i	1.139574i	1.141906i	3	1
1.288202i	1.271016i	1.266358i	1.266580i	2	2
1.470524i	1.623864i	1.536828i	1.518482i	4	0
1.574991i	1.713198i	1.622186i	1.623971i	3	2
1.606358i	1.739490i	1.681116i	1.658382i	4	1
1.769745i	1.772999i	1.731271i	1.732051i	0	3
1.894675i	1.857114i	1.789719i	1.790701i	1	3
	1.932489i	1.955014i	1.956130i	2	3

V. RESULTS

We implemented these techniques in software to compute the modes of arbitrarily-shaped, closed waveguides. Our code requires two inputs. The first is a description of the waveguide aperture. The aperture is described in terms of one or more quadrilateral or triangular patches. The mesh always covered the planar waveguide aperture exactly in order to preserve the ability to achieve high-order convergence in the solution. We locate discretization points on each of these patches according to a high-order $2d$ quadrature rule. Discretization points on the boundary are located according to a $1d$ quadrature rule of the same order. The number of such points is determined by the second input, the order of the quadrature rule. This value also determines the maximum order of the testing functions used to compute local corrections. The output of the code consists of numerically computed eigenmodes and eigenvalues.

We have tested the code by using it to compute modes of several waveguides with simple cross sections. Sample results for two waveguides are presented in this section. The first is a rectangular waveguide, a problem for which analytical solutions are available. We compare computed propagation constants (eigenvalues) to analytical results. The second problem is a rectangular waveguide containing two square conductors. Such a waveguide has two TEM modes in addition to its TM and TE modes. We list computed propagation constants and plot the lowest modes. Similar results have been obtained on other waveguide shapes including circular waveguide, circular coaxial waveguide, and rectangular waveguide with septum.

Tables I and II list eigenvalues for an $a \times b$ rectangular waveguide with $a = 1.1\lambda$ and $b = 0.75\lambda$. For computational purposes the waveguide aperture was defined by a single rectangular patch. The first column of each table gives the eigenvalues computed using a 16-point, high-order quadrature rule, namely a product rule constructed from two $1d$ Gauss-Legendre rules each using 4 points. The second and third columns give the 16 lowest eigenvalues computed using high-order product rules involving 36 and 64 points, respectively.

The fourth column gives the exact values of the 16 lowest eigenvalues. The analytical solutions [2] for a rectangular waveguide are well known. The modes satisfying Dirichlet boundary conditions take the form

$$\varphi_{mn}(x, y) = \sin\left(m\pi\frac{x}{a}\right) \sin\left(n\pi\frac{y}{b}\right) \quad \text{for } m, n = 1, 2, 3, \dots \quad (42)$$

Similarly, the Neumann modes are

$$\psi_{mn}(x, y) = \cos\left(m\pi\frac{x}{a}\right) \cos\left(n\pi\frac{y}{b}\right) \quad \text{for } m, n = 0, 1, 2, \dots \quad (43)$$

Accordingly, the exact eigenvalues for both Dirichlet and Neumann boundary conditions are

$$\frac{\beta_{mn}}{k} = \sqrt{1 - \left(\frac{m}{2a}\right)^2 - \left(\frac{n}{2b}\right)^2}. \quad (44)$$

The last two columns show the values of m and n for each computed mode. Four Neumann modes and one Dirichlet mode are propagating modes, the rest are evanescent.

Not surprisingly, the lower the mode, the more accurate the eigenvalue for a given quadrature rule. With a 64

TABLE III
COMPUTED EIGENVALUES (β/k) VS. DISCRETIZATION FOR A $5\lambda \times 3\lambda$ WAVEGUIDE CONTAINING TWO INTERIOR CONDUCTORS

First 10 TM modes		First 10 TE modes	
4 x 4	6 x 6	4 x 4	6 x 6
0.899770	0.898954	0.996147	0.996122
0.889666	0.888867	0.991385	0.991335
0.880594	0.879772	0.986280	0.986221
0.877820	0.877004	0.985071	0.985030
0.866849	0.866051	0.968195	0.968162
0.858987	0.858275	0.957283	0.957146
0.824123	0.822946	0.948050	0.947774
0.814496	0.813010	0.946083	0.946051

point quadrature rule, the lowest eigenvalues are accurate to almost 6 digits. The higher the spatial frequency content of the mode, however, the lower the accuracy of the computed result. This is evident in the list of Dirichlet eigenvalues computed using a 16-point quadrature rule. It also holds in both cases for the higher modes that were computed² but are not shown in the tables.

The second sample problem is a $3\lambda \times 5\lambda$ rectangular waveguide containing two $1\lambda \times 1\lambda$ square conductors. Table III lists the computed eigenvalues for the first ten Dirichlet/TM and Neumann/TE modes of the guide. All computations were performed using a mesh consisting of thirteen $1\lambda \times 1\lambda$ patches arranged on a Cartesian grid. The columns labeled '4 x 4' and '6 x 6' give results for discretizations derived from 16-point and 36-point product rules, respectively. The accuracy of the results can be estimated from the fact that results computed from the different discretizations agree to better than 2 digits in the TM case and better than 3 digits in the TE case. As for the previous problem, however, the accuracy of the propagation constants for the other modes declines with increasing mode number.

Plots of the vector modes are given in Figures 1 through 5. Small arrows indicate the local direction of the (transverse component of the) electric field in the aperture. The background shading represents the corresponding scalar potential.

Figure 1 shows the two TEM modes of the guide. The first was derived from the solution to the $2d$ Laplace equation assuming a unit potential on the left interior conductor and zero potential on all other boundaries. The second plot is essentially its mirror image. The lowest eight TM modes are shown in Figures 2 and 3 and the lowest eight TE modes are shown in Figures 4 and 5.

²The number of computed modes in this case equals the number of quadrature points.

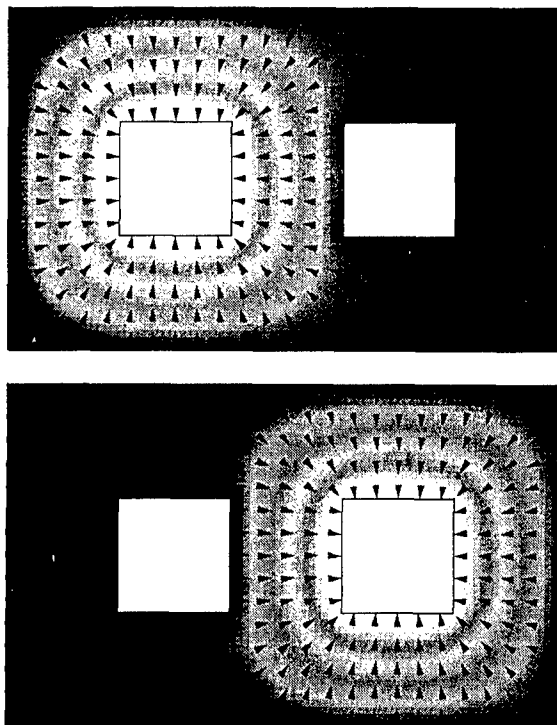


Fig. 1. TEM modes of a $5\lambda \times 3\lambda$ waveguide containing two interior conductors.

VI. CONCLUSIONS

Our method is based on the following observations: the scalar traveling modes of a waveguide can be obtained by diagonalizing an integral operator whose kernel is the Green function for the $2d$ scalar Helmholtz equation inside the waveguide aperture; the $2d$ electrostatic modes are solutions to the $2d$ Laplace equation inside the aperture; and, the electromagnetic modes can be obtained by taking gradients of these scalar modes.

We showed how to construct discretized representations of the various integral operators using the locally corrected Nyström method and presented results from a software implementation of this method.

Improvements are possible in a number of areas. For example, if we were to set up the $2d$ Laplace problem using a double-layer potential instead of a single-layer potential, the resulting integral equation would be second kind rather than first kind. Second kind integral equations are better conditioned and generally lead to more accurate solutions, especially for high spatial frequency modes. If we went one step further and combined the double layer potential with a single layer potential (i.e., employ a combined source formulation), the resulting equation would be second kind and would also be insensitive to spurious resonances. Similar considerations apply to the integral equations representing the Green

functions for the scalar traveling modes.

Our original objective was to compute an accurate, discretized representation of the waveguide integral equation³ in order to model waveguide apertures and excitations in general antenna and scattering problems. This requires accurate representations of the electromagnetic modes on the aperture. The results as presented here are not sufficiently accurate for this purpose. Consequently, this paper should be regarded as a report on a work in progress.

We are grateful for support from the Raytheon Company.

REFERENCES

- [1] L. S. Canino, J. J. Ottusch, M. A. Stalzer, J. L. Visher, and S. M. Wandzura, "Numerical solution of the Helmholtz equation in 2d and 3d using a high-order Nyström discretization," *Journal of Computational Physics*, vol. 146, pp. 627–663, 1998.
- [2] J. D. Jackson, *Classical Electrodynamics*. New York: John Wiley & Sons, second ed., 1975.
- [3] J. J. Ottusch, G. C. Valley, and S. Wandzura, "Integral equations and discretizations for waveguide apertures," *IEEE Transactions on Antennas and Propagation*, vol. 46, no. 11, pp. 1727–1738, 1998.
- [4] W. H. Press, B. P. Flannery, S. Teukolsky, and W. T. Vetterling, *Numerical Recipes — The Art of Scientific Computing*. Cambridge: Cambridge University Press, second ed., 1992.

³The waveguide integral equation [3] is an exact specification of the relationship between the transverse electric and magnetic fields in any cross section of a waveguide. When a waveguide takes part in a scattering problem, the waveguide integral equation plays the role of a (non-local) boundary condition relating \mathbf{E}_\perp and \mathbf{H}_\perp (or $\mathbf{M} \equiv \hat{\mathbf{n}} \times \mathbf{E}$ and $\mathbf{J} \equiv \hat{\mathbf{n}} \times \mathbf{H}$).

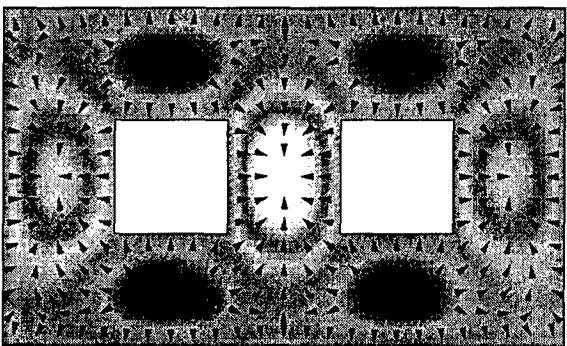
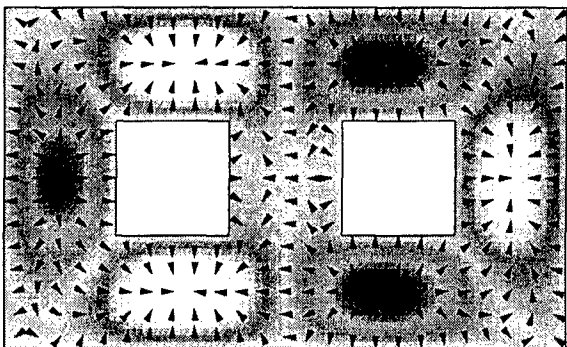
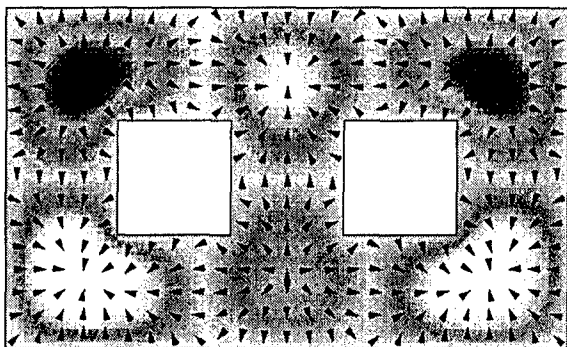
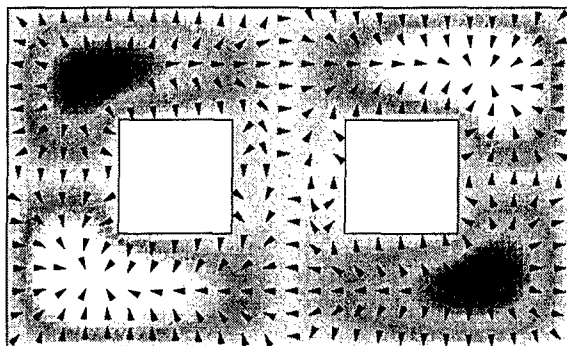
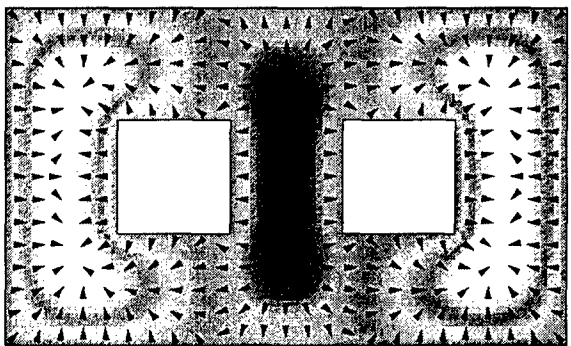
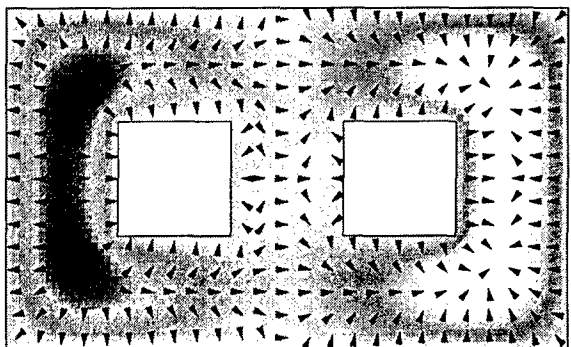
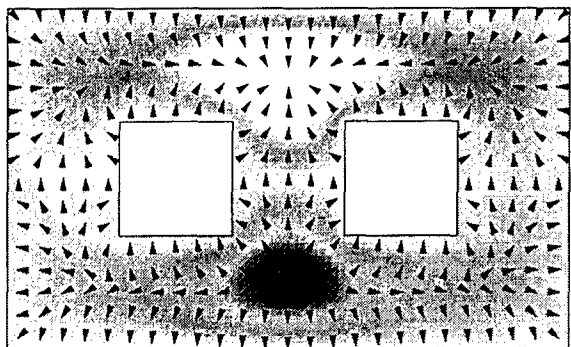
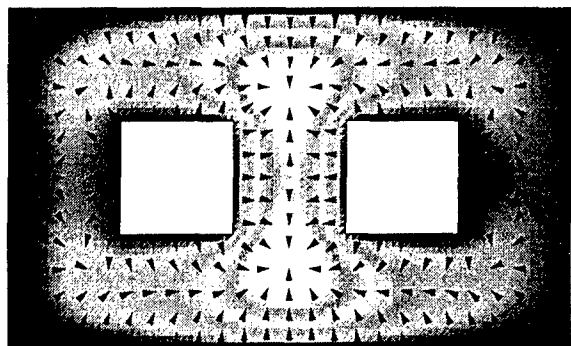


Fig. 2. First four TM modes of a $5\lambda \times 3\lambda$ waveguide containing two interior conductors.

Fig. 3. Second four TM modes of a $5\lambda \times 3\lambda$ waveguide containing two interior conductors.

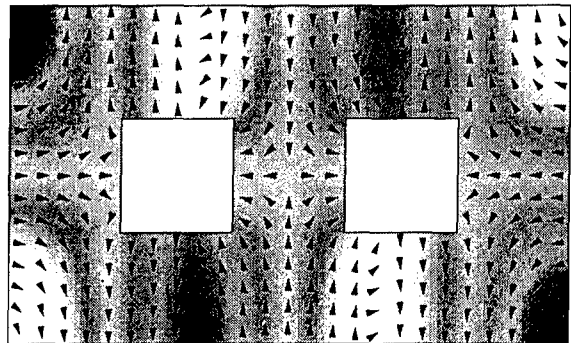
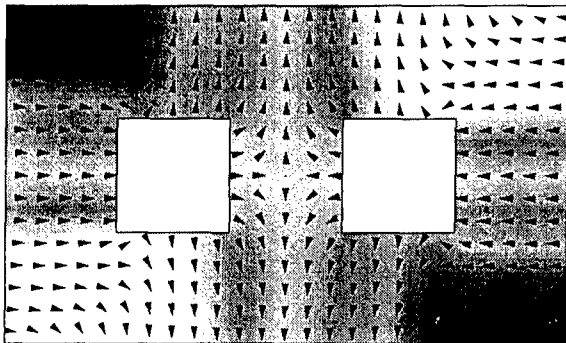
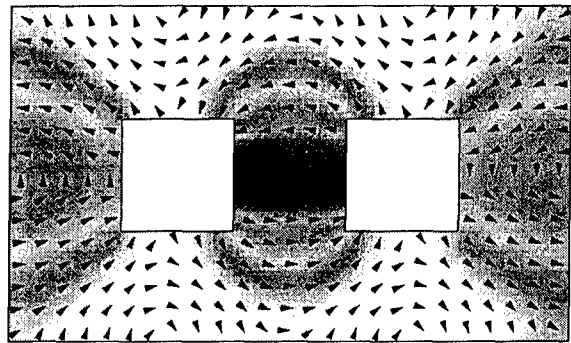
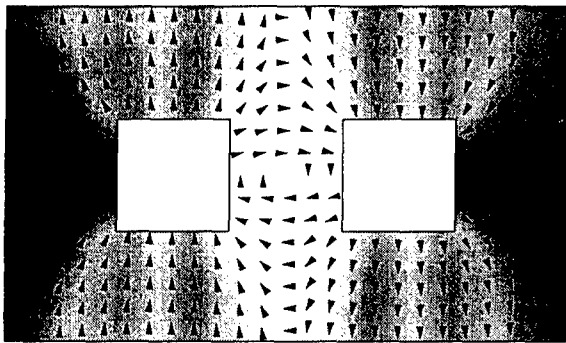
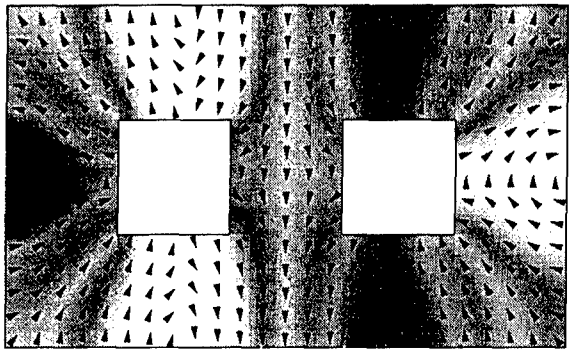
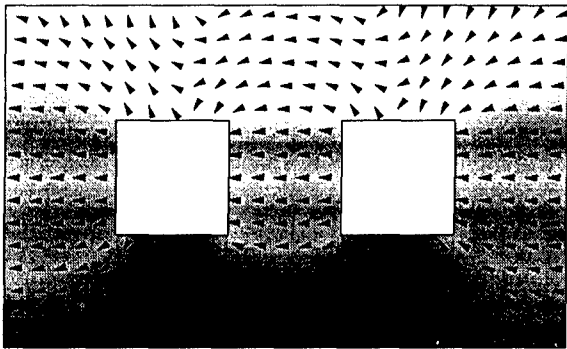
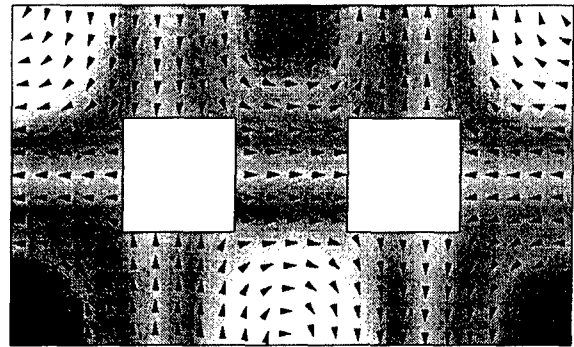
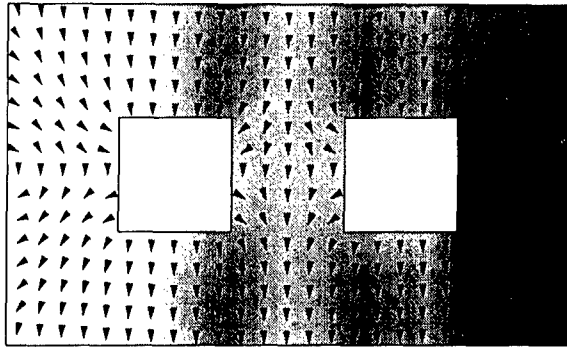


Fig. 4. First four TE modes of a $5\lambda \times 3\lambda$ waveguide containing two interior conductors.

Fig. 5. Second four TE modes of a $5\lambda \times 3\lambda$ waveguide containing two interior conductors.